Detection of Single Nanoparticles Using Photonic Crystal Enhanced Microscopy

Yue Zhuo[a], Huan Hu[b], Weili Chen[b], Meng Lu[b], Limei Tian[c], Hojeong Yu[b], Kenneth D. Long[a], Edmond Chow[d], William P. King[b,e,f], Srikanth Singamaneni[c], Brian T. Cunningham*[a,b,d]

[a] *Department of Bioengineering, University of Illinois at Urbana-Champaign, Urbana, Illinois 61801, USA*
[b] *Department of Electrical and Computer Engineering, University of Illinois at Urbana-Champaign, Urbana, Illinois 61801, USA*
[c] *Department of Mechanical Engineering and Materials Science, Washington University in St. Louis, St. Louis, Missouri 63130, USA*
[d] *Micro and Nanotechnology Laboratory, University of Illinois at Urbana-Champaign, Urbana, Illinois 61801, USA*
[e] *Department of Mechanical Science and Engineering, University of Illinois at Urbana-Champaign, Urbana, Illinois 61801, USA*
[f] *Department of Materials Science and Engineering, University of Illinois at Urbana-Champaign, Urbana, Illinois 61801, USA*
*E-mail: bcunning@illinois.edu

Abstract: We demonstrate a label-free biosensor imaging approach that utilizes a photonic-crystal surface to detect attachment of individual nanoparticles down to ~65×30×30nm^3. Matching nanoparticle plasmon resonant-frequency to the photonic-crystal resonance substantially increases sensitivity of the approach.

OCIS codes: (280.1415) Biological sensing and sensors; (050.5298) Photonic crystals; (170.3880) Medical and biological Imaging

1. Introduction

While many biosensing approaches are capable of sensing the adsorption of large numbers of nanoparticles (NP), several approaches can detect the presence of a single NP if it is adsorbed to a specific active location. Due to the difficulty of directing analytes to precise locations on a substrate surface where a biosensor has sensitivity, one approach to overcoming this limitation is to utilize a biosensor surface in which the entire surface area is active as a sensor (e.g. photonic crystal (PC) biosensors [1, 2]). We demonstrate the detection of single nanoparticles with photonic crystal enhanced microscopy (PCEM) [3] to image the attachment of dielectric and metallic nanoparticles upon a PC biosensor surface [4].

2. Photonic Crystal Enhanced Microscopy Design

A PC biosensor is a sub-wavelength grating structure consisting of a periodic arrangement of a low refractive index material coated with a high refractive index layer (Fig. 1a). Complete interference occurs on PC surface at a particular resonant wavelength and incident angle, resulting in nearly 100% reflection efficiency. The resonant wavelength can be modulated by the addition of biomaterial upon the PC surface that will cause a shift to the resonant reflection wavelength and resonance reflection efficiency. The electromagnetic standing wave generated at the PC surface during resonant light coupling effectively inhibits lateral propagation, enabling sensing of individual nanoparticles with submicron spatial resolution. By measuring the resonant peak wavelength value (PWV) and peak intensity value (PIV) on a pixel-by-pixel basis over a PC surface, an image of nanoparticle attachment may be recorded. The PC sensors (Fig. 1b, SEM image) can be fabricated using a low-cost nanoreplica molding approach [1]. The Lumerical Finite-Difference Time-Domain (FDTD) computer simulations of the PC structure demonstrate the distribution of electromagnetic fields (Fig. 1d) and local reflectance spectrum with resonant wavelength at ~620 nm (Fig. 1e) on the device surface. The PCEM system (Fig. 1c) is built upon the body of a standard microscope with a fiber-coupled LED illumination from below the PC at normal incidence. The reflected light is projected onto a spectrometer and then collected by a CCD camera. The PWV and PIV of each peak are determined by fitting the spectrum to a 2nd order polynomial and then mathematically determined as the maximum location (wavelength) and magnitude (intensity) of the function. To generate a 2D PWV or PIV image of the PC surface, a motorized stage translates the PC biosensor along the axis perpendicular to the imaged line and the same area on the PC surface can be scanned repeatedly over a long-term.

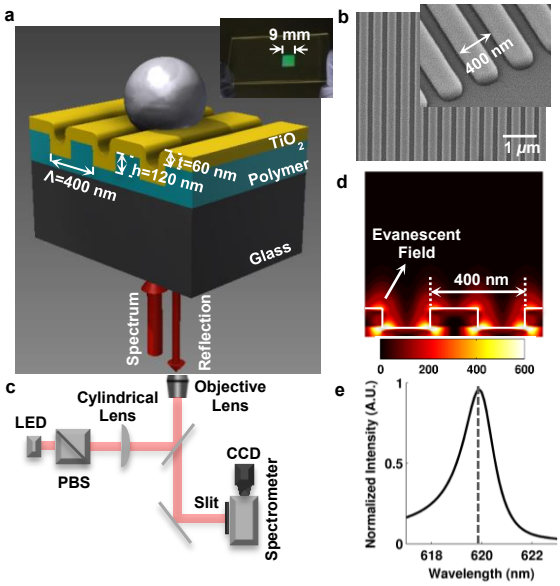

Fig.1 Principal of Photonic Crystal Enhanced Microscopy (PCEM). (a) Schematic diagram of a nanoparticle attached to a PC surface. Inset: Photo of a fabricated PC. (b) SEM image of the PC surface. (c) Instrument schematic of the PCEM. (d) The simulation (side view) of FDTD computed electric-field power distributions (units: V^2/m^2) of PC surface. (e) FDTD-computed reflection spectrum of PC biosensor surface.

3. Results and Discussion

To facilitate investigation of PCEM's ability to detect individual nanoparticles with tightly controlled spatial distribution and size, we first sought to intentionally deposit dielectric nano-patterns using thermal Dip-Pen Nanolithography (tDPN) [4] with a heated AFM tip to deposit polystyrene (PS) nano-dots on the PC surface. We printed 3×3 arrays of PS nano-dots (540 nm diameter, 40 nm height, and 5 µm gaps) on a PC surface confirmed by AFM imaging (Fig. 2a). Fig. 2b displays the measured PWV image of the tDPN printed nano-dots. From the spectra of two neighboring pixels (Fig. 2c), we can visualize a PWV shift of $\Delta\lambda = 0.5$ nm caused by the nano-dots compared to the background pixel. We next sought to detect dielectric TiO_2 NP of approximately the same size, but distributed randomly on the PC surface, which induces a highly localized PWV shift of $\Delta\lambda = 1.12$ nm and a PIV reduction of $\Delta I = 58\%$ (Fig. 2d-f).

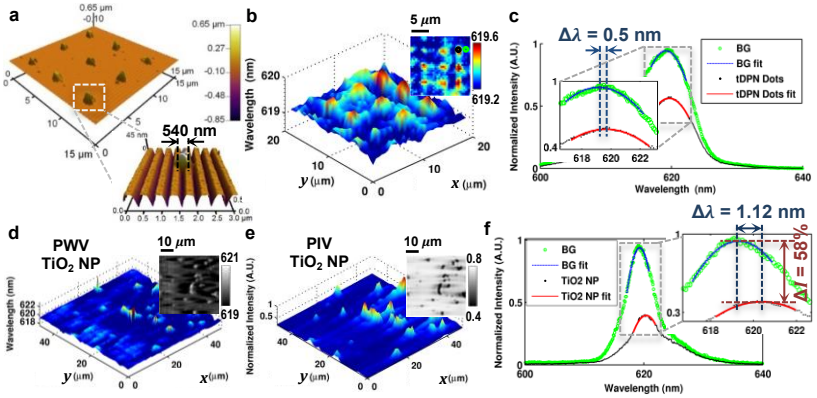

Fig. 2 PCEM detection of dielectric NP. (a) AFM images of tDPN-printed 3×3 arrays of nano-dots (540×540×40 nm^3). (b) PWV image of the tDPN nano-dots displayed in a 3D surface plot. (c) Normalized spectrum of a representative tDPN nano-dot (black line) and a background pixel (green line). (d) PWV and (e) PIV images of randomly distributed TiO_2 NP (3D surface plot). (f) Normalized spectra of a TiO_2 NP and a background pixel.

Additionally, we studied the biosensor's ability to detect target bioanalytes binding with immobilized antibody on the PC biosensor surface with metal nanoparticles as tags. To match the PC resonant wavelength, we synthesized gold nanorods (AuNR, 65×30×30 nm^3) with resonant optical absorption spectra around ~620 nm [4]. Then we employed Rabbit IgG as model capture biomolecule and anti-Rabbit IgG as model target bioanalyte to demonstrate the detection of antibody-antigen binding (Fig. 3a). The AuNR-IgG conjugates were prepared by functionalizing AuNRs with SH-PEG-IgG molecules (SH-PEG is a hydrophilic polymer, serves as a flexible linker). Subsequently, anti-IgG was adsorbed onto the PC biosensor surface, and then exposing the PC surface to AuNR-IgG conjugates. This resulted in specific binding of AuNP-IgG to anti-IgG (SEM image shown in Fig. 3b), which can be detected as a PIV reduction in the area absorbed with AuNR-IgG. Fig. 3c shows the mathematical difference between two PIV images taken before and after AuNR-IgG attachment and the selected cross-section lines in the PIV images (Fig. 3d). It demonstrates that PCEM can successfully detect the intensity reduction in presence of AuNR-IgG.

4. Conclusions

In conclusion, we report the first application of PCEM system to the detection of individual surface-adsorbed nanoparticles (65×30×30 nm^3) with highly localized shift in the PC's reflected resonant wavelength and resonant reflection efficiency. We envision the development of sandwich-style assays in which the PC surface is prepared with capture molecules for low-concentration analytes (such as cancer biomarkers), where nanoparticle tags prepared with secondary antibodies can decorate the captured analyte. Such an approach may enable multiplexed detection of analytes with single-molecule resolution in the future.

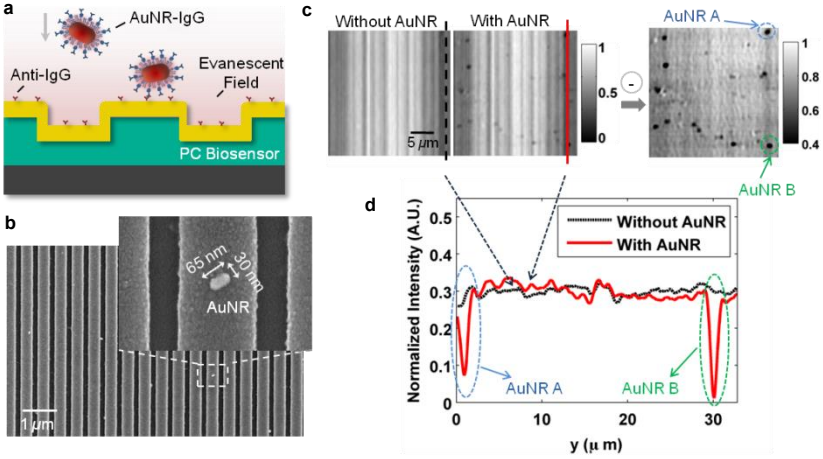

Fig. 3 PCEM detection of protein-protein binding with metal NP. (a) Schematic illustration of AuNR-IgG attachment on the PC biosensor surface. (b) SEM images of AuNR-IgG attached to the PC surface. (c) PIV images and the difference between without and with AuNR-IgG. (d) Two cross-section lines of the PIV images with/without AuNR-IgG.

References

[1] B. T. Cunningham, B. Lin, J. Qiu, P. Li, J. Pepper and B. Hugh, *Sensor Actuators B-Chem*, 2002, 85, 219-226..
[2] B. T. Cunningham, P. Li, B. Lin and J. Pepper, *Sensor Actuators B-Chem*, 2002, 81, 316-328.
[3] W. Chen, K. D. Long, M. Lu, V. Chaudhery, H. Yu, et al., *Analyst*, 2013, 138, 5886-5894.
[4] Y. Zhuo, H. Hu, W. Chen, M. Lu, L. Tian, et al., *Analyst,* DOI: 10.1039/c3an02295a.